Surface reactivity of amphibole asbestos: A comparison between two tremolite samples with different surface area

Alessandro Pacella [1,*], Giovanni B. Andreozzi [1,2], Ingrid Corazzari [3,4], Maura Tomatis [3,4], Francesco Turci [3,4]

[1] Department of Earth Sciences, Sapienza University of Rome, P.le A. Moro 5, I-00185 Rome, Italy
[2] CNR-IGAG, U.O. Roma, at Department of Earth Sciences, Sapienza University of Rome, P.le A. Moro 5, I-00185 Rome, Italy
[3] Department of Chemistry, University of Torino, via Pietro Giuria 7, I-10125 Torino, Italy
[4] "G. Scansetti" Interdepartmental Centre for Studies on Asbestos and Other Toxic Particulates, University of Torino, via Pietro Giuria 9, I-10125 Torino, Italy

ARTICLE INFO

ABSTRACT

Surface reactivity of a fibrous tremolite sample from Castelluccio Superiore (Italy) was investigated by means of free radical generation following incubation in H_2O_2 solution buffered at pH 7.4, for several time points, ranging from 1 day to 1 month. Results obtained were compared with those of another fibrous tremolite sample (from Maryland, USA), with much smaller surface area.

Structural, morphological, and chemical alterations induced on tremolite by incubation were investigated by HR-TEM/EDS. The generation of $HO^{\bullet}$ and $COO^{-\bullet}$ radicals following reaction of tremolite with H_2O_2 or formate ion was investigated by spin trapping/EPR spectroscopy.

The dissolution process and surface modification were slower for the Maryland sample, with lowest surface area. Surface modification indicated the occurrence of either low- or high-coordinated Fe centres on the surface, as well as the evolution of their nuclearity. In turn, iron centres determine the reactivity of the fibre surface and the yield of $HO^{\bullet}$ and $COO^{-\bullet}$ radical species. The evolution of radical reactivity over time was proved to be largely dependent on surface area, with the highest radical yield occurring for low-area tremolite incubated over long times. The experimental results obtained in this study as well as the comparison with previous studies further confirm that surface reactivity of mineral fibres and inorganic particles is not dependent on Fe_{tot} content per se, but is likely due to surface properties and occurrence of specific iron sites.

Keywords: asbestos; tremolite; dissolution; surface reactivity; radical generation; nanoparticles; Electron Paramagnetic Resonance (EPR) Spectroscopy; High-Resolution Transmission Electron Microscopy (HR-TEM).

INTRODUCTION

Interactions between human respiratory system and mineral particles (dusts, fibres, etc.) are governed by particle morphological and physico-chemical parameters, including size, biopersistence and surface chemistry. It is widely recognized that the toxicity of respirable mineral particles may largely differ according to their physical and chemical properties (see for example Fubini et al., 2011). Among the breathable hazardous particles, asbestos are by far the most recognized and investigated. Asbestos is a group of six naturally-occurring silicate minerals encompassing one fibrous serpentine (chrysotile) and five

fibrous amphibole (anthophyllite, tremolite, actinolite, riebeckite, and grunerite, with the last two commercially known as crocidolite and amosite, respectively). Asbestos-containing materials have been widely used in the past and their use is now virtually discontinued worldwide. Chrysotile is banned or strictly regulated in EU, US, China and most developed countries, while is still extracted and used in many emerging economies (Kazan-Allen, 2016). In the natural environment, fibrous amphiboles and chrysotile are frequently found associated in ophiolitic rock complexes, where non-hydrostatic stress field favoured the formation of the asbestiform habit. When these rocks are excavated or weathered (e.g., in soils), human exposure to asbestiform amphibole in its natural setting may occur (Turci et al., 2016). Epidemiological studies have clearly shown that exposure (both occupational and non-occupational) to all kind of asbestos may induce severe respiratory diseases, including malignancies as mesothelioma and lung cancer (Gunter et al., 2007; Donaldson and Seaton, 2012).

Despite an extraordinary research effort, the complex molecular interaction between asbestos fibres and lung tissue has not been fully elucidated yet (Liu et al., 2013; Pascolo et al., 2013; Gandolfi et al., 2016). It is widely held that high aspect ratio (that is the length divided by the width), biodurability and surface chemical reactivity of the fibres are the three main factors in determining the pathological response to asbestos, with thin fibres being able to reach the alveolar region, the deepest portion of the lung (e.g., Stanton et al., 1981). There, asbestos surface chemistry (in turn determining fibre durability and reactivity) contributes to macrophage activation and tissue damage (Kamp and Weitzman, 1999). This paradigm holds for many hazardous inhaled particles and fibres (Hochella, 1993; Fubini et al., 1995; Hohr et al., 2002; Fubini et al., 2011; Turci et al., 2015). Asbestos chemical reactivity received considerable attention by the biomedical community and was undoubtedly related to the presence and bioavailability of Fe (Bonneau et al., 1986). The most robust mechanism-based structure-activity relationship for asbestos includes generation of iron-mediated reactive oxygen species (ROS) (Fubini and Otero-Areàn, 1999; Shukla et al., 2003; Gazzano et al., 2007). Both the presence and the structural coordination of Fe were shown to be crucial factors of chrysotile asbestos toxicity (Turci et al., 2011). Furthermore, only the Fe on the fibre surface, and in particular Fe^{2+}, was considered to play a primary role for the ROS production from amphiboles asbestos (Hardy and Aust, 1995; Pacella et al., 2010, 2012; Fantauzzi et al., 2010, 2012). Two biologically relevant reactions, which might yield the formation of radical species, are commonly exploited to investigate the chemical nature of the exposed iron ions at the surface of asbestos fibres (Fubini et al.,

1995). In the first one, H_2O_2 reacts with surface ferrous iron (Martra et al., 2003) producing hydroxyl radical $HO^{\bullet}$ in a Fenton-like reaction:

$$Fe^{2+}_{surf} + H_2O_2 \rightarrow Fe^{3+}_{surf} + OH^- + HO^{\bullet} \qquad \text{1a)}$$
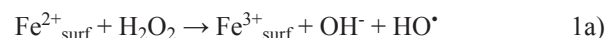
The release of the hydroxyl radical in the presence of hydrogen peroxide is held to occur in vivo when asbestos fibres are exposed to lysosomal fluids during alveolar macrophage phagocytosis (particle-induced direct oxidative stress). The reaction may take place also in the presence of ferric iron, that can be reduced to ferrous iron with production of superoxide radical $O_2^{-\bullet}$ (Tomatis et al., 2002):

$$Fe^{3+}_{surf} + H_2O_2 \rightarrow Fe^{2+}_{surf} + 2H^+ + O_2^{-\bullet} \qquad \text{1b)}$$
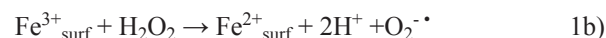
The iron-related reactivity of asbestos is also investigated with formate ion as target molecule, with the cleavage of the C-H bond employed as a model reaction that may occur to several molecules of biological interest such as peptides, proteins and lipids. Such a reaction yields the formation of a carbon-centred radical $COO^{-\bullet}$:

$$HCOO^- \xrightarrow{Fe^{2+}/Fe^{3+}} COO^{-\bullet} + H \qquad \text{2a)}$$

where direct surface-assisted homolytic cleavage possibly occurs on redox-reactive iron. Alternatively, or even complementarily, highly reactive hydroxyl radical promotes the homolytic cleavage of the C-H bond in formate anion:

$$HCOO^- + HO^{\bullet} \rightarrow H_2O + COO^{-\bullet} \qquad \text{2b)}$$

Iron content of the various amphibole asbestos is very different, with anthophyllite and tremolite as the lowest and riebeckite (crocidolite, in its fibrous form) and grunerite (amosite) at the highest end. Scientists have for a long time searched for a quantitative relationship between the amount of iron and asbestos toxic potency. Nonetheless, tremolite asbestos is considered to be more toxic than iron-rich amphibole asbestos (Wagner et al., 1982; Weill et al., 1990; Case, 1991; Nolan et al., 1991; Srivastava et al., 2010), questioning if iron total content could be a real proxy for chemical reactivity and, lastly, for toxicity of asbestos. Very recently, a study performed by our group on the pathogenic-related surface reactivity of fibrous amphiboles (crocidolite and tremolite) showed that the radical production is dependent on specific surface Fe sites rather than the total Fe content of the minerals (Andreozzi et al., 2017). In particular, both ferrous and ferric iron with one or more unsaturated coordinative valences are involved in the Fenton and Fenton-like

reactions with hydrogen peroxide, which yield HO•
radical, while Fe centres with two or more unsaturated
coordinative bonds are responsible for the production
of COO$^{-•}$ radical from formate anion. Moreover, the
investigation of the chemical reactivity after sample
leaching in oxidative medium buffered at pH 7.4 (up to
one month) demonstrated that both fibrous amphiboles
have sustained radical production, even when highly
altered by oxidative leaching (Andreozzi et al., 2017).

The present study represents a step forward toward
the understanding of the molecular role of the specific
surface area when dealing with mineral reactivity. The
investigated tremolite sample (coming from Castelluccio
Superiore, Italy) was previously fully characterised in
terms of bulk chemistry (including bulk Fe oxidation
state), crystal chemistry, and surface chemistry (including
surface Fe oxidation state and aggregation state) by using
ICP-OES, EMP, XRPD, HR-TEM, EDS, Mössbauer
spectroscopy and X-ray Photoelectron spectroscopy
(Fantauzzi et al., 2010; Pacella et al., 2010, 2014, 2015).
The fibres of Castelluccio tremolite were incubated in
H_2O_2 solution buffered at pH 7.4 for several time points,
ranging from 1 day to 1 month. Even being far from
mimicking a real cellular environment, such conditions
have been chosen to promote the dissolution dynamics in
a reasonable experimental time. Structural and chemical
characterization of both untreated and leached fibres have
been carried out by means of high resolution transmission
electron microscopy (HR-TEM) and energy dispersive
spectroscopy (EDS), respectively. The generation of HO$^•$
and COO$^{-•}$ radical species over time has been investigated
by spin trapping/EPR spectroscopy. Results obtained
on Castelluccio sample have been compared with those
previously obtained by Andreozzi et al. (2017) on another
fibrous tremolite sample with different surface area.

This work proposes a correlation between chemical
reactivity and the dissolution model of fibrous amphiboles
(as defined in Pacella et al., 2014, 2015), focusing on the
role of surface properties. The proposed approach, yet
mechanistic and simplified in nature, may also contribute
to understand the unexpectedly high toxicity of fibrous
tremolite, in spite of its very low Fe content.

EXPERIMENTAL
Materials

The fibrous tremolite investigated in this work comes
from ophiolitic outcrops of Castelluccio Superiore
(Basilicata, Potenza, Italy). This sample will be compared
with another fibrous tremolite from ophiolitic outcrops
in Maryland (Montgomery County, Maryland, United
States), previously studied by Pacella et al. (2010).

Surface area and textural analysis were obtained by
N_2 adsorption/desorption measurements at the liquid

nitrogen temperature (-196 °C) using a 3-Flex analyser
(Micromeritics, Norcross, GA, USA), on the basis of
Brunauer-Emmett-Teller (BET) multipoint method
(Gregg and Sing, 1982). Surface area is 10.07 m^2g^{-1} for
Castelluccio and 2.75 m^2g^{-1} for Maryland.

The chemical, structural and spectroscopic
characterization of the two fibrous tremolite samples was
obtained by using a multi-analytical approach including
EMP, XRPD and Mössbauer spectroscopy data (Pacella
et al., 2010). The only chemical difference between them
is that Maryland sample has a Fe_{tot} content higher than
Castelluccio (4.50 and 2.06 wt%, respectively). In both
samples Fe^{2+} is highly dominant over Fe^{3+} ($Fe^{2+}\sim80\%$
Fe_{Tot}). The retrieved structural formulae are:

$$^B(Ca_{1.87}Na_{0.06}K_{0.01}Mn_{0.01}Mg_{0.05})_{\Sigma2.00}{}^C(Mg_{4.79}Fe^{2+}{}_{0.19}$$
$$Mn_{0.01}Fe^{3+}{}_{0.05}{}^{VI}Al_{0.01})_{\Sigma5.05}{}^T(Si_{7.99}Al_{0.01})_{\Sigma8.00}O_{22}{}^{O(3)}$$
$$(OH_{1.97}F_{0.02})_{\Sigma1.99}$$

for Castelluccio Superiore sample (hereafter called
Castelluccio), and

$$^B(Ca_{1.99}Na_{0.01}Mn_{0.02})_{\Sigma2.02}{}^C(Mg_{4.48}Fe^{2+}{}_{0.44}$$
$$Mn_{0.02}Fe^{3+}{}_{0.08}{}^{VI}Al_{0.01})_{\Sigma5.03}{}^T(Si_{7.95}Al_{0.01})_{\Sigma7.96}O_{22}{}^{O(3)}$$
$$(OH_{1.97}F_{0.01})_{\Sigma1.98}$$

for Maryland sample.

Both samples show a crystal-chemical formula and
a cation ratio very close to those of the ideal tremolite,
$^BCa_2{}^CMg_5{}^TSi_8O_{22}{}^{O3}(OH)_2$ and Ca/ΣM=0.4 (where ΣM=
Mg+Fe^{2+}+Mn+Ni+Ti+^{VI}Fe^{3+}+^{VI}Cr^{3+}+^{VI}Al).

If not stated differently, all reagents were from Sigma-
Aldrich (Milan, Italy). Ultrapure Milli-Q water (Merck-
Millipore, Vimondrone, Italy) was used throughout.

Fibre incubation in buffered solution at pH 7.4

Experimental conditions of fibre incubation were those
reported in Pacella et al. (2014, 2015) for dissolution
experiment performed on the same samples of this work
and previously adopted for chemical reactivity tests
(Pacella et al., 2012). In particular, 25 mg of fibres were
suspended in 2 ml of a hydrogen peroxide (0.1 M) solution
buffered with potassium phosphate (KPB, 0.5 M, pH 7.4)
and incubated for 24 h, 48 h, 168 h (1 week) and 720 h (1
month). The suspensions were continuously shaken in a
thermostatic oscillating bath at 37 °C. To recover the fibres
from the tubes, the samples were centrifuged at 10000×g
for 10 min and then rinsed with 2 ml of Milli-Q ultrapure
deionised water for 3 times prior to reactivity tests.

EPR measurement of HO$^•$ production

The ability of both untreated and incubated samples to
generate HO$^•$ radical in presence of H_2O_2 via a surface-
driven Fenton-like reaction was evaluated using Electron
Paramagnetic Resonance (EPR) spectroscopy following

a well-established procedure (Fubini et al., 1995). All tests were performed at 37 °C in absence of light. The mixture contained 25 mg of sample, 500 µl of 0.5 M potassium phosphate buffer solution (pH 7.4), and 250 µl of DMPO (5,5-dimethyl-1-pyrroline-N-oxide, Cayman chemical company, Ann Arbor, USA) as spin trapping agent (0.18 M). The reaction was triggered adding 250 µl of H_2O_2 solution (0.2 M). The vial was placed on a magnetic stirrer to ensure the homogeneity of the suspension. For both untreated and incubated samples a fraction of the suspension was drawn after 10, 30, and 60 minutes, filtered through cellulose acetate membranes (porosity 0.2 µm) and transferred into a 50 µl-capillary tube. All spectra were recorded on a Miniscope MS 100 (Magnettech, Berlin, Germany) EPR spectrometer. The instrument settings were as follows: microwave power, 10 mW; modulation, 1 G; scan range, 120 G; centre of field, approximately 3375 G. Experiments were performed in duplicate and blanks were performed in parallel in the absence of fibres. The number of radicals released is proportional to the intensity of the EPR signal measured by double integration.

EPR measurement of COO⁻˙ production

The ability of both untreated and incubated samples to generate carbon-centred ($COO^{-\bullet}$) radicals from the homolytic cleavage of the C-H bond in the formate ion was investigated by EPR spectroscopy. Experiments were conducted both in presence and in absence of ascorbic acid. All tests were performed at 37 °C and in absence of light. The reaction mixture contained 25 mg of sample, 250 µl of DMPO (0.18 M), 500 µl of sodium formate (2M) in phosphate buffer (1 M, pH 7.4) and 250 µl of distilled water or ascorbic acid (3 mM). Ascorbic acid was added to the reaction mixture to reduce surface iron ions. The experiments were carried out as previously described for $HO^{\bullet}$ radical measurements.

HR-TEM investigation

The structural and morphological alteration induced on tremolite fibres by incubation in hydrogen peroxide buffered solution were monitored after 24 h, 48 h and 1 month. Characterisation of untreated and incubated samples after 1 week are reported in Pacella et al. (2014, 2015). Samples were investigated by JEOL 3010-UHR High-Resolution Transmission Electron Microscopy (HR-TEM) with a LaB_6 filament operated at 300 KeV, beam current 114 µA and equipped with a 2K x 2K pixels Gatan US1000 CCD camera. Elemental analysis was performed by Oxford INCA X-ray energy dispersive spectrometer (X-EDS) with a Pentafet Si(Li) detector. The fibres were dispersed in ultrapure MilliQ water, sonicated for 20 minutes and a droplet was deposited on lacey carbon Cu grids.

RESULTS
Structural and morphological alterations of leached fibres

Results of HR-TEM investigation on Castelluccio tremolite fibres incubated in H_2O_2/KPB at pH 7.4, for 24h, 48h, and 1 month, are presented and discussed together with results obtained by Pacella et al. (2015) on the same pristine fibres and on those incubated for one week in identical experimental conditions.

Pristine tremolite samples showed bundles of long and thin fibres with micrometric to nanometric width (≥100 nm). At higher magnification, several thinner sub-micrometric fibres consisting of associated single-crystal nanometric fibrils revealing a perfect amphibole cleavage along c axis could be observed for all pristine amphiboles (Pacella et al., 2015).

TEM results obtained on Castelluccio tremolite revealed that after 24 h of treatment in the hydrogen peroxide buffered solution the fibres, included the thinnest fibrils, persisted unaltered (Figure 1a). High-resolution TEM image of the fibril highlighted the unaffected crystalline lattice of tremolite (Figure 1b, inset). Additionally, EDS analysis excluded significant chemical alteration. After 48 h of leaching, crystalline structure of surface layers resulted partially modified, with the occurrence of few punctual modifications and the initial formation of amorphous phases (Figure 1c). High resolution images revealed the presence of an incipient amorphous layer surrounding the fibres (Figure 1c, inset). However, EDS spectra did not show a significant modification with respect to pristine fibres. After 1 month of incubation, patches of altered material surrounded the fibres (Figure 1d). High resolution images unveiled that, though tremolite structure was preserved, some neo-formed amorphous nanoparticles occurred on top of the fibres (Figure 1d, inset).

In addition, results of HR-TEM investigation on Maryland tremolite fibres (Andreozzi et al., 2017) are here reported for comparison purposes. Similarly to Castelluccio, the Maryland fibres resulted largely unaltered after 24 h of leaching (Figure 2b). Notably, tremolite structure of the Maryland sample was still highly preserved after 48 h of leaching and even after 1 month (Figures 2 c,d). The incipient formation of few altered nanometric clusters were only occasionally observed on the 48h-leached sample, while large patches of amorphous areas were detected on the fibre surface after 1 month of incubation (Figure 2d, inset).

Free radical generation of leached asbestos fibres

The surface reactivity of Castelluccio tremolite fibres leached with hydrogen peroxide/KBP solution at different time points was evaluated by means of two radical tests, namely the production of hydroxyl radicals ($HO^{\bullet}$) via
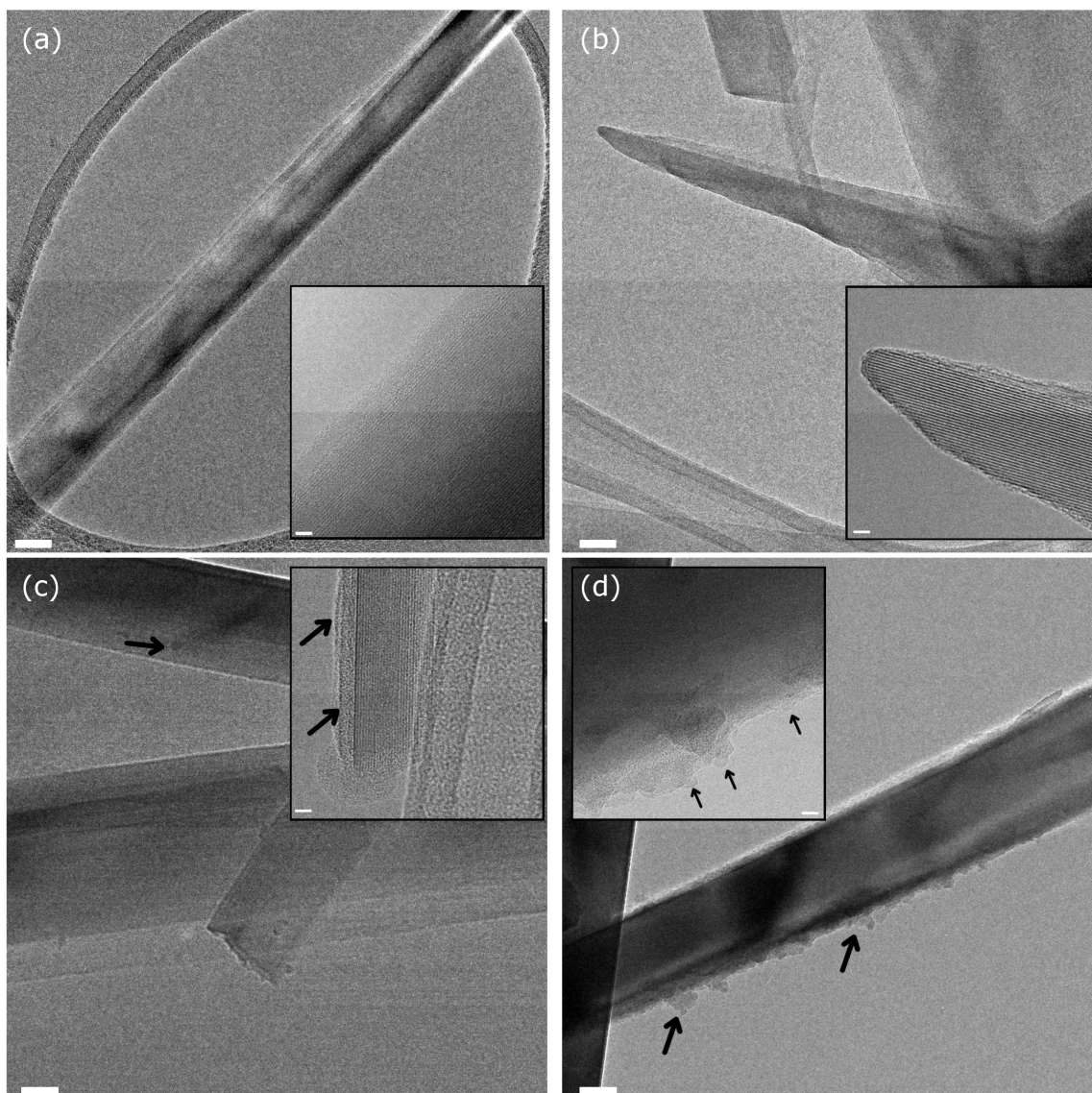
Figure 1. Representative TEM images of untreated and 24, 48 and 720 hour leached tremolite from Castelluccio (a,b,c, and d, respectively). Amorphous layers and nanoparticles are evidenced with black arrows throughout the figure. Relative scale bars: 50 nm, main pictures; 5 nm, high-resolution inset.

Fenton and Fenton-like reactions (reaction 1 a,b), and the production of carbon-centred radicals (COO$^{-\bullet}$) via the cleavage of the C-H bond of formate anion (reaction 2 a,b). To quantify the amount of radical generated, EPR spectra were analysed and each EPR spectrum was double-integrated as described in previous works (Fubini et al., 1995; Turci et al., 2011). Adopting the approach of Andreozzi et al. (2017), for every incubation time the total amount of radicals released during the first hour of reaction with the target molecule (H_2O_2 or formate anion) was summed up (Table 1). Surface reactivity results obtained on Maryland tremolite by Andreozzi et al. (2017) are reported for comparison purposes.

Generation of HO$^{\bullet}$

Results obtained on Castellucio tremolite show that surface reactivity for the long-leached fibres is lower than that of the untreated ones (Figure 3). In particular, a significant decrease of the hydroxyl radical production is observed in the first 24 h (from 137 to 80 a.u.) Notably, the same trend was observed for Maryland tremolite fibres, whose radical production decreased, even in a larger amount (from 218 to 55 a.u.), in the same interval of time (Andreozzi et al., 2017).

However, a different trend is observed for the intermediate leaching time points, with the radical yield of Castelluccio tremolite rising up and attaining a plateaux
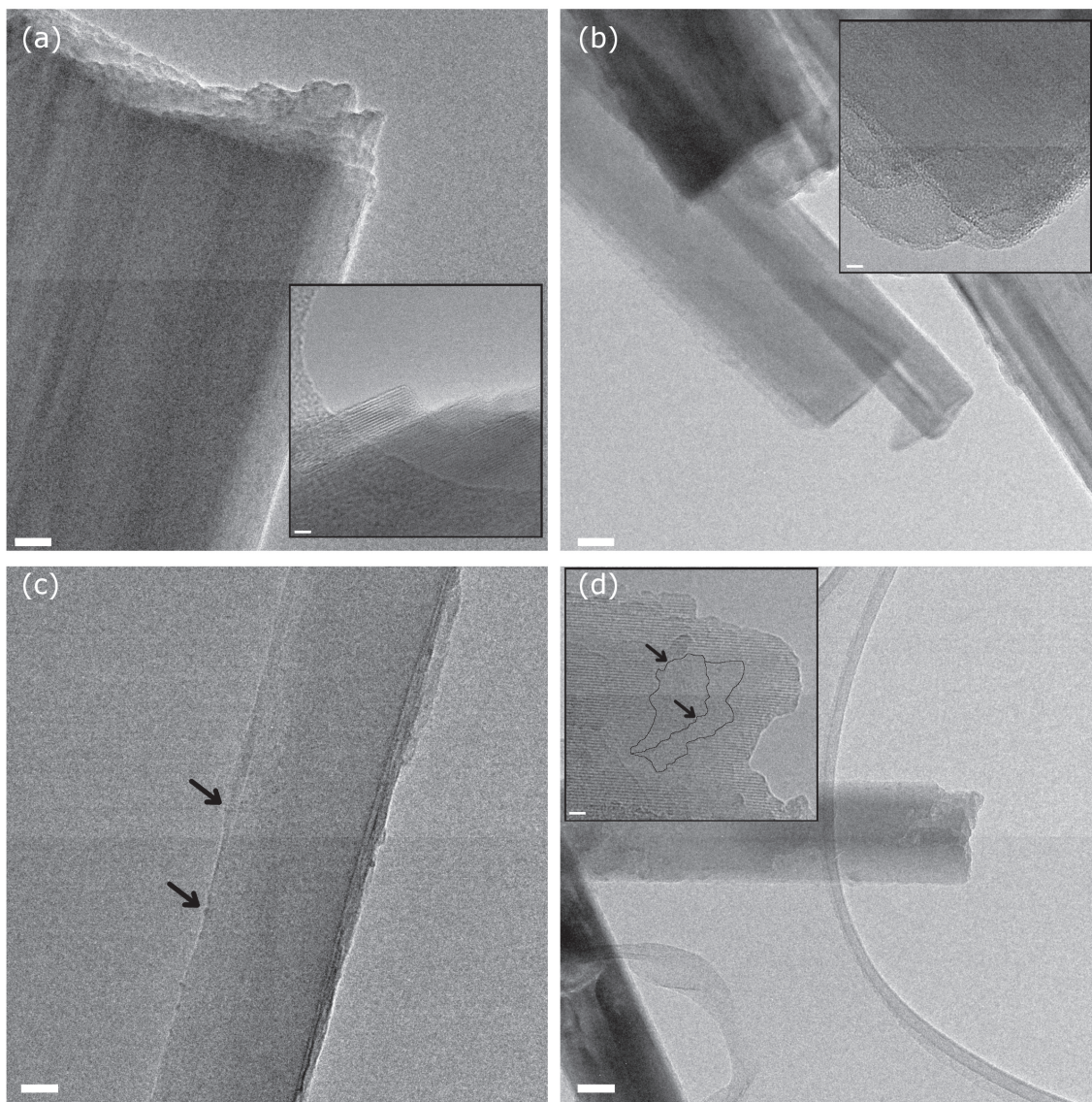
Figure 2. Representative TEM images of untreated and 24, 48 and 720 hour leached tremolite from Maryland (a,b,c, and d, respectively; from Andreozzi et al., 2017). Large patches of amorphous layers are evidenced with black arrows in section d, inset. Relative scale bars: 50 nm, main pictures; 5 nm, high-resolution inset.

already after 48 h (Figure 3a), and that of Maryland tremolite slowly increasing up to 1 month, and possibly more (Figure 3b).

Generation of $COO^{\bullet}$

To test the fibre ability to induce the homolytic cleavage of the C-H bond, ascorbic acid -one of the major components of the antioxidants defences in the aqueous phase of the alveolar lining layer (Willis and Kratzing, 1976)- was added to the reaction mixture to promote the reduction of redox-active centres at the surface. This was done because no radical production had been observed for both pristine and leached samples in absence of ascorbic acid (data not shown).

Results evidence that the $COO^{\bullet}$ production of Castelluccio tremolite keeps almost constant for the first 24 h (64 a.u.), but suddenly peaks up after 48 h (ca. 215 a.u.), and then continuously decreases up to 1 month (Figure 4a).

Conversely, Maryland tremolite exhibited the maximum $COO^{\bullet}$ radical production in absence of leaching (i.e., untreated sample, ca. 117 a.u.), followed by an abrupt suppression after 24 h (Andreozzi et al., 2017). However, the radical yield was restored after 48 h (ca. 75 a.u.), and

Table 1. Total radical amount (HO$^\bullet$ and COO$^{-\bullet}$) obtained from Castelluccio tremolite. Standard deviations (in brackets) were calculated over two measurements. Data of Maryland tremolite (Andreozzi et al., 2017) are reported for comparison.

		Castelluccio tremolite	Maryland tremolite
total DMPO-HO$^\bullet$ production	t = 0	173 (13)	218 (22)
	t = 24 h	80 (9)	5 (10)
	t = 48 h	113 (19)	55 (4)
	t = 168 h	119 (4)	60 (9)
	t = 720 h	97 (12)	117 (6)
total DMPO- COO$^{-\bullet}$ production	t = 0	75 (13)	117 (10)
	t = 24 h	64 (3)	n.d.
	t = 48 h	215 (18)	n.d.
	t = 168 h	122 (2)	75 (3)
	t = 720 h	37 (1)	95 (15)

then slightly increased up to the longest leaching time (Figure 4b).

DISCUSSION

The most remarkable difference between Castelluccio tremolite and Maryland sample is the surface area, that of the former being almost four times that of the latter and this will be one of the most important factors to explain their behaviour. Actually, there is also a small difference of their iron contents, that of Castelluccio tremolite being half that of Maryland, but among asbestos such a difference is negligible if compared with Fe content of UICC crocidolite, almost twenty times higher (Pacella et al., 2014). The alteration pathway of tremolite fibres here observed by HR-TEM is in perfect agreement with the multi-step mechanism described in Pacella et al. (2015). In that paper it has been demonstrated that amphibole asbestos alteration (in a H$_2$O$_2$ buffered solution at pH=7.4) occurs following several steps: an incongruent dissolution of the amphiboles takes place in the first stages of surface alteration resulting in an amorphous, altered surface layer; iron oxidation and formation of FeOOH species may take place together with the congruent dissolution of the altered layer; insoluble Fe-rich oxide clusters and larger amorphous nanoparticles on top of the fibres are eventually formed in the last stages. For the two tremolite samples, the higher surface area of Castelluccio with respect to Maryland produced a faster leaching process that leaded to the formation of insoluble Fe-rich nanoparticles (Figure 1 b-d).

Before leaching, pristine fibres of Castelluccio tremolite, in spite of its higher surface area, exhibited a lower radical production compared to that measured for Maryland (Figures 3 and 4). In particular, for both HO$^\bullet$ and COO$^{-\bullet}$ radical species, pristine Castelluccio tremolite showed a chemical reactivity reduced by a factor of 1.6 with respect to Maryland, and this behaviour is paralleled by reduced surface Fe contents (0.9 at% for Castelluccio and 1.4 at% for Maryland, as measured by XPS by Fantauzzi et al., 2010 and Pacella et al., 2015). Accordingly, this is an evidence that chemical reactivity of the two samples is directly related to Fe centres concentration at their surfaces. However, some "saturation effect" should be also taken into account. In fact, comparable production of both HO$^\bullet$ and COO$^{-\bullet}$ radicals was observed when pristine UICC crocidolite and Maryland tremolite were compared, in spite of iron contents of crocidolite almost ten times (Andreozzi et al., 2017). Notably, Lim et al. (2006) showed that the catalytic activity for heterogeneous Fenton reactions of iron oxide nanoparticles (immobilized in alumina coated mesoporous silica) increased for Fe content ranging from 3 wt% to 6 wt%, but decreased for Fe content up to 24 wt%.

Fenton-like surface reactivity and generation of HO$^\bullet$ over time

For Castelluccio and Maryland samples, the evolution of the Fenton-like surface reactivity with time (Figure 3) can be tentatively linked to the incipient fibre alteration observed by HR-TEM (Figures 1 and 2). For Castelluccio, the early surface modification is driven by its higher surface area, which determines a relatively faster leaching during incubation (Pacella et al., 2015). Accordingly, we can consider the alteration process related to Maryland tremolite as a "slow-motion" of the very first steps of the dissolution and surface modification process, the entire development of which may be observed analysing Castelluccio sample. This assumption nicely correlates
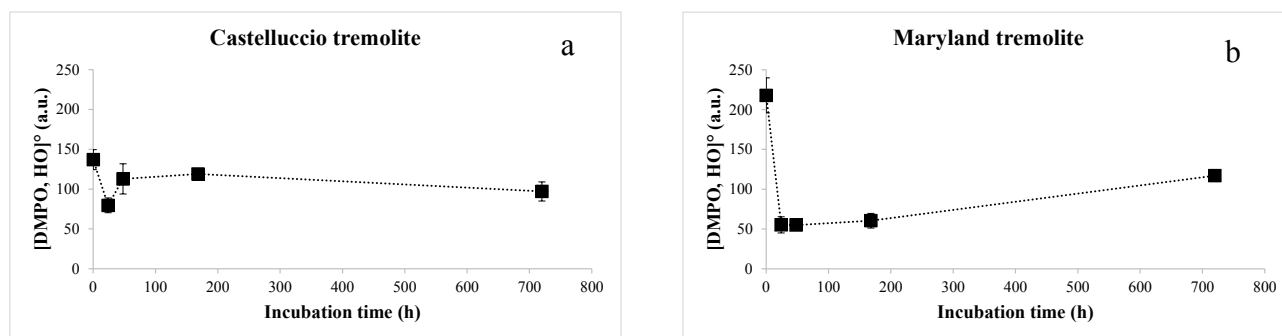
Figure 3. Total [DMPO-OH]• production (arbitrary units, a.u.) of the investigated asbestos samples as a function of the incubation time (0, 24, 48, 168, 720 h) for: a) Castelluccio tremolite, and b) Maryland tremolite.
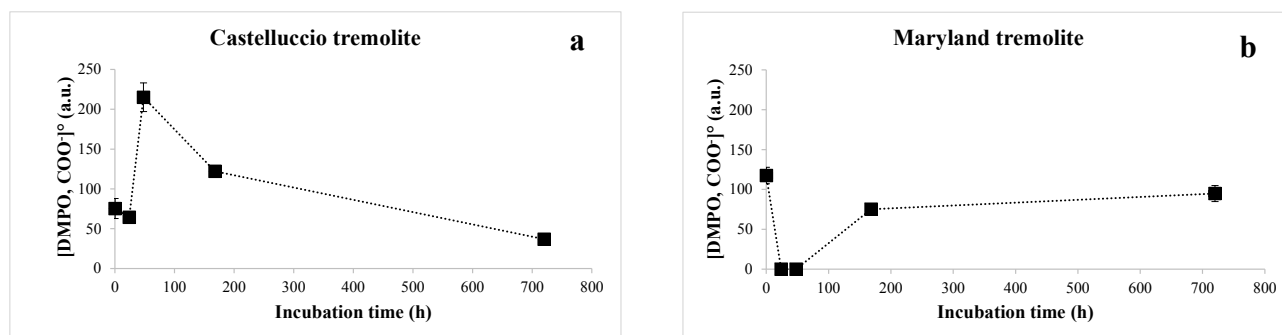

Figure 4. Total [DMPO-COO⁻]• production (arbitrary units, a.u.) of the investigated asbestos samples in presence of ascorbic acid as a function of the incubation time (0, 24, 48, 168, 720 h) for: a) Castelluccio tremolite, and b) Maryland tremolite.

with the HO• radical kinetics displayed by the two fibres upon leaching, so that the entire reactivity pathway exhibited by Maryland should correspond to the first 48 hour path shown by Castelluccio (Figure 3). Moreover, the reduction in HO• radical production observed for the leached fibres with respect to the pristine ones corresponds to a sudden decrease of surface Fe centres able to interact with hydrogen peroxide, followed by a prompt (for Castelluccio) or sluggish (for Maryland) reactivity rejuvenation. Notably, this behaviour is opposite to that displayed by crocidolite, for which the observed increase in the Fenton-like activity over time was related to its quicker dissolution (compared to that of tremolite) and to the continuous occurrence on the fibre surface of new Fe centres rising from the Fe-enriched bulk (Andreozzi et al., 2017).

Cleavage of the C-H bond and generation of COO⁻• over time

Both for pristine and leached fibres COO⁻• radical release was only observed in presence of ascorbic acid, a well-known reducing agent. This result implies that most of the iron ions exposed at the very first surface atomic layers is oxidized and is subsequently reduced by ascorbic

acid, as the yielding of COO⁻• radical was reported to be strongly dependent on the presence of ferrous iron at the fibre surface (Turci et al., 2011). Such a conclusion is in line with previous studies, as the ferric oxidation state is thermodynamically favoured by the oxidative action of chemical weathering (Pacella et al., 2015) or of thermal treatments (Tomatis et al., 2002), and the use of ascorbic acid was essential to obtain COO⁻• radical production by fibrous amphiboles (Andreozzi et al., 2017). The evolution with time of the reactivity towards formate anion suggests that, also in this case, the behaviour exhibited by Maryland tremolite may be considered as a "slow-motion" of that of Castelluccio (Figure 4). Therefore, keeping in mind that the higher surface area of Castelluccio tremolite with respect to Maryland is the cause for the quicker surface alteration during leaching (Figures 1, 2), the structure-reactivity paradigm adopted so far implies that the faster dissolution kinetics of Castelluccio likely promotes the removal of the first atomic layers (especially in the first 48 hours, see Pacella et al., 2015 for details). Accordingly, for Castelluccio tremolite the occurrence on the surface of low-coordinated Fe centres (i.e., ions bearing two coordinative position not occupied by structural ligands)

has to be responsible for the enhanced COO⁻• radical activity observed between 0-48h (Figure 4a). In fact, it was pointed out that only the low-coordinated ferric ions may effectively interact with ascorbic acid to be reduced and therefore become active in the homolytic cleavage of the C-H bond in formate anion (Suter et al., 1991). On the contrary, for Maryland the replacement of low-coordinated Fe^{3+} ions by high-coordinated-ones (i.e., ions bearing only one coordinative position not occupied by structural ligands) was considered by Andreozzi et al. (2017) the cause of the complete suppression of COO⁻• radical production observed within 24-48 h (Figure 4b). After 48 h, for Castelluccio tremolite the progressive appearance of Fe nanoparticles on the fibre surface (Figure 1d) has to be related with the decrease of its reactivity towards formate (Figure 4a). Namely, the faster dissolution of Castelluccio tremolite and the consequent removal of surface layers likely caused the aggregation of insoluble Fe centres into nanoparticles, which determined a "passivation" of the surface and justify the partial reduction of reactivity. Notably, Pham et al. (2009) claimed that the aggregation of low coordinated iron into clusters alters the number and properties of the reactive surface sites. Accordingly, Pacella et al. (2017) showed that only Fe (III) residing at the fibres surface and characterized by low nuclearity is significantly reduced by ascorbic acid. On this basis, the sluggish leaching of Maryland sample was considered by Andreozzi et al. (2017) the key to produce isolated low-coordinated Fe centres which restored the COO⁻• production (Figure 4b).

CONCLUSIONS

The experimental results obtained in this study as well as the comparison with previous studies further confirm that surface reactivity of mineral fibres and inorganic particles is not dependent on total Fe content, but is likely due to surface properties and specific iron sites. In particular, for samples with low total Fe contents, a direct correlation between radical production and Fe centres concentration at their surfaces was observed, but the opposite is expected for samples with high total Fe contents.

The comparison between two fibrous tremolite samples with largely different surface area revealed that both the processes of dissolution and surface modification are slower for the sample with lowest surface area. Notably, the sample with lowest surface area exhibited during one month a sluggish chemical reactivity evolution, likely corresponding to the first 48 hour reactivity evolution shown by the sample with highest surface area.

Kinetics of fibre dissolution and surface modification was found to rule the occurrence of either low-coordinated or high-coordinated Fe centres on the surface, as well as the nuclearity of those Fe centres (preventing or enhancing the formation of clusters and nanoparticles). All these factors control the interactions of fibre surface with hydrogen peroxide and ascorbic acid, finally determining the actual production of HO• and COO⁻• radical species. Over long times, it can be expected that the samples with a low surface area are more efficient to generate radical species, making these fibres potentially more toxic than those with a high surface area.

REFERENCES

Andreozzi G.B., Pacella A., Corazzari I., Tomatis M., Turci F., 2017. Surface reactivity of amphibole asbestos: a comparison between crocidolite and tremolite. Scientific Reports 7, doi:10.1038/s41598-017-14480-z.

Bonneau L., Suquet H., Malard C., Pezerat H., 1986. Studies on surface properties of asbestos. 1. Active sites on surface of chrysotile and amphiboles. Environmental Research 41, 251-267.

Case B.W., 1991. Health effects of tremolite. In: The third wave of asbestos disease: Exposure to asbestos in place. Landrigan PJ, Kazemi H eds., Annals of the New York Academy of Sciences 63, 491-504.

Donaldson K. and Seaton A., 2012. A short history of the toxicology of inhaled particles. Particle and Fibre Toxicology 9, p.13.

Fantauzzi M., Pacella A., Atzei D., Gianfagna A., Andreozzi G.B., Rossi A., 2010. Combined use of X-Ray Photoelectron and Mössbauer spectroscopic techniques in the analytical characterization of iron oxidation state in amphibole asbestos. Analytical and Bioanalytical Chemistry 396, 2889-2898.

Fantauzzi M., Pacella A., Fournier J., Gianfagna A., Andreozzi G.B., Rossi A., 2012. Surface chemistry and surface reactivity of fibrous amphibole that are not regulated as asbestos. . Analytical and Bioanalytical Chemistry 404, 821-833.

Fubini B. and Otero-Arean, C., 1999. Chemical aspects of the toxicity of inhaled mineral dusts. Chemical Society Reviews 28, 373-381.

Fubini B., Fenoglio I., Tomatis M., Turci F., 2011. Effect of chemical composition and state of the surface on the toxic response to high aspect ratio nanomaterials. Nanomedicine 6, 899-920.

Fubini B., Mollo L., Giamello E., 1995. Free radical generation at the solid/liquid interface in iron containing minerals. Free Radical Research 23, 593-614.

Gandolfi N.B., Gualtieri A.F., Pollastri S., Tibaldi E., Belpoggi F., 2016. Assessment of asbestos body formation by high resolution FEG-SEM after exposure of Sprague-Dawley rats

to chrysotile, crocidolite, or erionite. Journal of Hazardous Materials 306, 95-104.

Gazzano E., Turci F., Foresti E., Putzu M.G., Aldieri E., Silvagno F., Lesci I.G., Tomatis M., Riganti C., Romano C., Fubini B., Roveri N., Ghigo D., 2007. Iron-Loaded Synthetic Chrysotile: A New Model Solid for Studying the Role of Iron in Asbestos Toxicity. Chemical Research in Toxicology 20, 380-387.

Gregg S.J. and Sing K.S.W., 1982., Adsorption, Surface Area and Porosity. Second Edition, Academic Press.

Gunter M.E., Belluso E., Mottana A., 2007. Amphiboles: Environmental and Health Concerns, in: F.C. Hawthorne R., Oberti G., Della Ventura A., Mottana (Eds.). Amphiboles: Crystal Chemistry, Occurrence, and Health Issues. Reviews in Mineralogy and Geochemistry 67, 453-516.

Hardy J.A. and Aust A.E., 1995. Iron in asbestos chemistry and carcinogenicity. Chemical Reviews 118, 95-97.

Hochella M.F., 1993. Health Effects of Mineral Dust. Reviews in Mineralogy and Geochemistry 28, 275-308.

Hohr D., Steinfartz Y., Schins R.P., Knaapen A.M., Martra G., Fubini B., Borm P.J., 2002. The surface area rather than the surface coating determines the acute inflammatory response after instillation of fine and ultrafine TiO_2 in the rat. I International Journal of Hygiene and Environmental Health 205, 239-244

Kamp D.W. and Weitzman S.A., 1999. The molecular basis of asbestos induced lung injury. Thorax 54, 638-652.

Kazan-Allen L., 2016. International Ban Asbestos Secretariat (IBAS), http://ibasecretariat.org/asbestos_ban_list.php.

Lim H., Lee J., Jin S., Kim J., Yoon J., Hyeon T., 2006. Highly active heterogeneous Fenton catalyst using iron oxide nanoparticles immobilized in alumina coated mesoporous silica. Chemical Communications 4, 463-465.

Liu G., Cheresh P., Kamp D.W., 2013. Molecular basis of asbestos-induced lung disease. Annual Review of Pathology 8, 161-187.

Martra G., Tomatis M., Fenoglio I., Coluccia C., Fubini B., 2003. Acid Modifies the Surface of Asbestos: Possible Implications in the Molecular Mechanisms of Toxicity. Chemical Research in Toxicology 16, 328-335.

Nolan R.P., Langer A.M., Oechsle G.W., Addison J., Colflesh D.E., 1991. Association of tremolite habit with biological potential: Preliminary report. In: Mechanisms in Fibre Carcinogenesis. Brown RC, Hoskins JA, Johnson NF (eds) Plenum Press, New York, 231-251.

Pacella A., Andreozzi G.B., Fournier J., 2010. Detailed crystal chemistry and iron topochemistry of asbestos occurring in its natural setting: a first step to understanding its chemical reactivity. Chemical Geology 277, 197-206.

Pacella A., Andreozzi G.B., Fournier J., Stievano L., Giantomassi F., Lucarini G., Rippo M.R., Pugnaloni A., 2012. Iron topochemistry and surface reactivity of amphibole asbestos: relations with in vitro toxicity. Analytical and Bioanalytical

Chemistry 402, 871-881.

Pacella A., Fantauzzi M., Turci F., Cremisini C., Montereali M.R., Nardi E., Atzei D., Rossi A., Andreozzi G.B., 2014. Surface modifications and dissolution reactions of UICC crocidolite in buffered solutions at physiological pH: a combined ICP-OES, XPS and TEM investigation. Geochimica et Cosmochimica Acta 127, 221-232.

Pacella A., Fantauzzi M., Turci F., Cremisini C., Montereali M.R., Nardi E., Atzei D., Rossi A., Andreozzi G.B., 2015. Surface alteration mechanism and topochemistry of iron in tremolite asbestos: a step toward understanding the potential hazard of amphibole asbestos. Chemical Geology 405, 28-38.

Pacella A., Fantauzzi M., Atzei D., Cremisini C., Nardi E., Montereali M.R., Rossi A., Ballirano P., 2017. Iron within the erionite cavity and its potential role in inducing its toxicity: evidences of Fe (III) segregation as extra-framework cation. Microporous and Mesoporous Materials 237, 168-179.

Pascolo L., Gianoncelli A., Schneider G., Salomé M., Schneider M., Calligaro C., Kiskinova M., Melato M., Rizzardi C., 2013. The interaction of asbestos and iron in lung tissue revealed by synchrotron-based scanning X-ray microscopy. Scientific Reports 3, 1123.

Pham A.L.T., Lee C., Doyle F.M., Sedlak D.L., 2009. A Silica-Supported Iron Oxide Catalyst Capable of Activating Hydrogen Peroxide at Neutral pH Values. Environmental Science and Technology 43, 8930-8935.

Shukla A., Gulumian M., Hei T.K., Kamp D., Rahman Q., Mossman B.T., 2003. Multiple roles of oxidants in the pathogenesis of asbestos-induced diseases. Free Radical Biology and Medicine 34,1117-1129.

Srivastava R.K., Lohani M., Pant A.B., Rahman Q., 2010. Cyto-genotoxicity of amphibole asbestos fibers in cultured human lung epithelial cell line: role of surface iron. Toxicology and Industrial Health 26, 575-582.

Stanton M.F., Layard M., Tegeris A., Miller E., May M., Morgan E., Smith A., 1981. Relation of particle dimension to carcinogenicity in amphibole asbestoses and other fibrous minerals. Journal of the National Cancer Institute 67, 965-975.

Suter D., Banwart S., Stumm, W., 1991. Dissolution of Hydrous Iron(III) Oxides by Reductive Mechanisms. Langmuir 7, 809-813.

Tomatis M., Prandi L., Bodoardo S., Fubini B., 2002. Loss of surface reactivity upon heating amphibole asbestos. Langmuir 18, 4345-4350.

Turci F., Tomatis M., Lesci I.G., Roveri N., Fubini B., 2011. The iron-related molecular toxicity mechanism of synthetic asbestos nanofibres: a model study for high-aspect-ratio nanoparticles. Chemistry 17, 350-358.

Turci F., Corazzari I., Alberto G., Marta G., Fubini B., 2015. Free-radical chemistry as a means to evaluate lunar dust health hazard in view of future missions to the moon. Astrobiology 15, 371-380.

Turci F., Favero-Longo S.E., Gazzano C., Tomatis M., Gentile-Garofalo L., Bergamini M., 2016. Assessment of asbestos exposure during a simulated agricultural activity in the proximity of the former asbestos mine of Balangero, Italy. Journal of Hazardous Materials 308, 321-327.

Wagner J.C., Chamberlain M., Brown R.C., Berry G., Pooley F.D., Davies R., Griffiths D.M,. 1982. Biological effects of tremolite. British Journal of Cancer 45, 352.

Weill H., Abraham J.L., Balmes J.R., Case B., Chrug A., Hughes J., Schenker M., Sebastien P., 1990. Health effects of tremolite. American Review of Respiratory Disease 142, 453-1458.

Willis R.J. and Kratzing C.C., 1976. Extracellular ascorbic acid in lung. Biochimica et Biophysica Acta 444, 108-111.